Molecular dynamics simulation of paracetamol molecules ordering around glycogen

Wilber Lim, Yuan Ping Feng, and X. Y. Liu
Department of Physics, Faculty of Science, National University of Singapore, 2 Science Drive 3, Singapore 117542, Singapore
(Received 2 August 2004; revised manuscript received 2 January 2005; published 9 May 2005)

By the use of classical atomistic molecular dynamics simulations, we demonstrate that paracetamol molecules exist in a highly ordered phase in the presence of a glycogen substrate at 317 K whereas the paracetamol fluid exists in an isotropic phase in the absence of the glycogen substrate at the same temperature. This result further validates the studies made on polysaccharide regarding its abilities to promote nucleation of paracetamol via liquid preordering. As little is known regarding liquid ordering induced by a polymeric substrate, we seek to explore the ordering mechanism from an energy perspective. This is accomplished using conformation mappings. Our analysis shows that the conformation space accessible to the paracetamol molecule at 317 K in the vicinity of glycogen is smaller than the one in the absence of glycogen. An investigation on the orientation of the dipole moments of the glycogen monomers and paracetamol molecules were carried out as well. From the investigations, we show that dipolar interactions play an important role in the ordering process. These studies bear significance to the understanding of the ordering process as well as the promotion and effective control of the nucleation rate.

DOI: 10.1103/PhysRevE.71.051604 PACS number(s): 68.47.Pe, 05.65.+b, 07.05.Tp

I. INTRODUCTION

Nucleation is a kinetic process in which embryos overcome a nucleation barrier ΔG^* to reach a critical radius r_c and develop as crystals at a positive thermodynamics driving force $\Delta\mu/kT$, where $\Delta\mu$, is the difference between the chemical potentials of the solute molecules in the fluid phase and the solid phase, k is the Boltzmann constant, and T is temperature [1]. The effective promotion or inhibition of nucleation is important in many important technologies such as epitaxial growth, nanoparticle self-assembly, and macromolecular crystallization. One method to promote nucleation is to either lower the nucleation barrier or facilitate the kink kinetics in terms of inducing the preordering of fluid molecules at the interface with the use of substrates. As both effects normally occur simultaneously, the verification of the second effect is not easy. However, it is possible to remove the first effect, known as the interfacial nucleation barrier lowering effect by choosing a substrate with $R' = R_s/r_c \ll 1$, where R_s refers to the radius of the substrate. Certain polymers such as polysaccharide can be regarded as substrate of this type. Recent studies [2] have shown that polysaccharide strands are able to reduce the orientational and conformational free energy barrier for the kink incorporation of paracetamol molecules by inducing a certain degree of preordering.

The determination of a cheap and effective polymeric substrate that promotes the nucleation of anesthetic molecules can translate into cost reduction for the pharmaceutical industry which relies on supersaturation and batch cooling techniques for the crystallization of crude paracetamol. Better control of the nucleation process can be achieved using a polymeric substrate. However, little is known regarding the preordering process at the molecular level. As a result, it is necessary to investigate how complex anesthetic molecules such as paracetamol can adopt the required orientation and conformation required by the crystal structure in the presence of a substrate with $R' \ll 1$, in this particular case, polysaccharide. An identification of the mechanism for the ordering process will serve to advance our understanding of nucleation control. Molecular dynamics (MD) simulation is a suitable choice for such an investigation. In this paper, we seek to understand the mechanism of preordering by a polymeric substrate through the use of molecular dynamics and conformational mappings. Based on the computational studies, we have also constructed a model that will allow us to determine the orientation of anesthetic molecules in the presence of polysaccharides.

II. METHODS

A. Force field

We chose the consistent valence forcefield [3] (CVFF) for the evaluation of the potential energy function and atom typing due to its applicability in handling a wide range of organic systems. Atomic charges for the various atoms of glycogen and paracetamol are presented in Table I.

B. Initial structures

The choice of polysaccharide is arbitrary. We constructed an all-atom model of glycogen oligomer comprising of five monomers to represent the polysaccharide substrate. The structures of paracetamol and glycogen (Fig. 1) were generated using InsightII software. Each paracetamol molecule consists of 20 atoms and the glycogen oligomer consists of 108 atoms.

As we expect significant ordering within a short distance from the glycogen strand, five paracetamol molecules were placed near the polysaccharide (atomic coordinates are not given in this paper). The low density of paracetamol molecules provides us a better means of isolating the ordering mechanism due to the polysaccharide substrate. In other words, the correlation between neighboring paracetamol molecules can be reduced significantly. Furthermore, as we

TABLE I. Partial charges of selected atoms.

Glycogen atom ID	Partial charge	Paracetamol atom ID	Partial charge
*C*1	0.200	*C*1	−0.100
*C*2	−0.070	*C*2	−0.100
*C*3	−0.070	*C*3	0.030
*C*4	−0.070	*C*4	−0.100
*C*5	0.050	*C*5	−0.100
*C*6	−0.170	*C*6	0.100
O	−0.300	*C*8	0.380
*O*1	−0.300	*C*10	−0.300
*O*2	−0.380	*N*8	−0.390
*O*3	−0.380	*O*7	−0.380
*O*6	−0.380	*O*11	−0.380

shall see later, the presence of polysaccharide induces the ordered phase of paracetamol molecules despite the fact that low density favors the isotropic phase. Both the *cis* and *trans* conformers (with respect to the phenylene and methyl groups) of the paracetamol molecules were included [4]. Solvation effects are modeled explicitly by adding water molecules. In total, 2030 water molecules were added. To avoid edge effects and the influence of image polysaccharides on the ordering of paracetamol molecules, a $40\times40\times40$ Å unit cell with periodic boundary conditions imposed was used to contain the paracetamol molecules, glycogen and water molecules. In all, there are 6298 atoms. The system is then optimized using Discover with the cell size constrained. Figure 2 shows the result of energy minimization.

A smaller system comprising of only paracetamol molecules and water molecules was constructed in the same way. The two systems are identical in all respect except that one contains a glycogen molecule and the other does not. The purpose is to study the ordering of paracetamol, if any, in the absence of a glycogen substrate at room temperature.

C. Simulations

For energy minimization and the subsequent dynamical simulation, nonbond interactions are calculated using a group-based summation method with a cutoff of 15.5 Å.

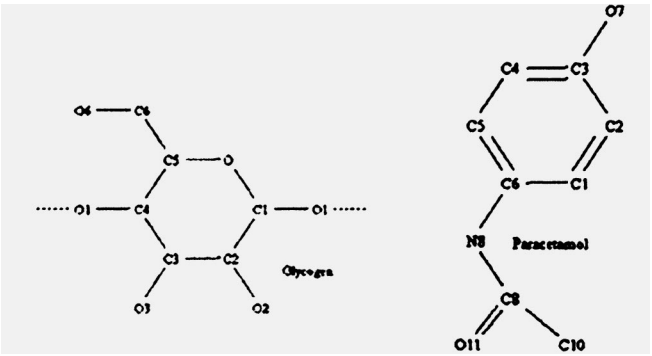

FIG. 1. Chemical structure of glycogen and paracetamol (hydrogen atoms are omitted from these diagrams). Discussions in later sections will adopt the labels used in this figure.

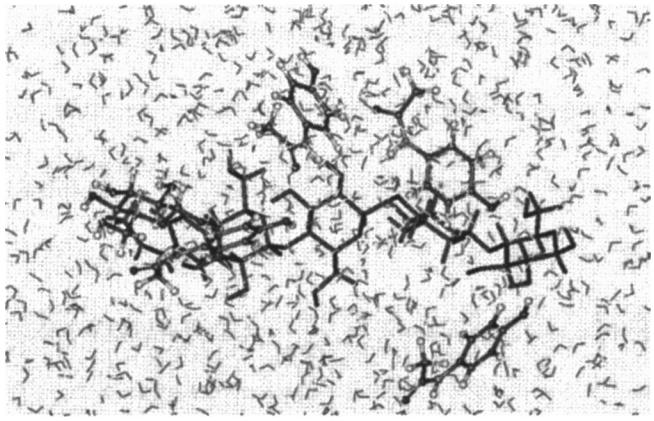

FIG. 2. Paracetamol and glycogen conformations after energy minimization. 1, 2, 4–6: Paracetamol molecules. 3: Glycogen.

Spline width and buffer width are set at 1.0 and 0.5 Å, respectively. No constraint on the bonds was applied. The time step is 1 fs.

To allow for faster equilibration, the temperature T for the system was raised to 600 K before reducing it to 317 K. This is shown in Fig. 3 with $T=2E_k/3Nk_B$. Temperature is kept constant using the direct velocity-scaling scheme:

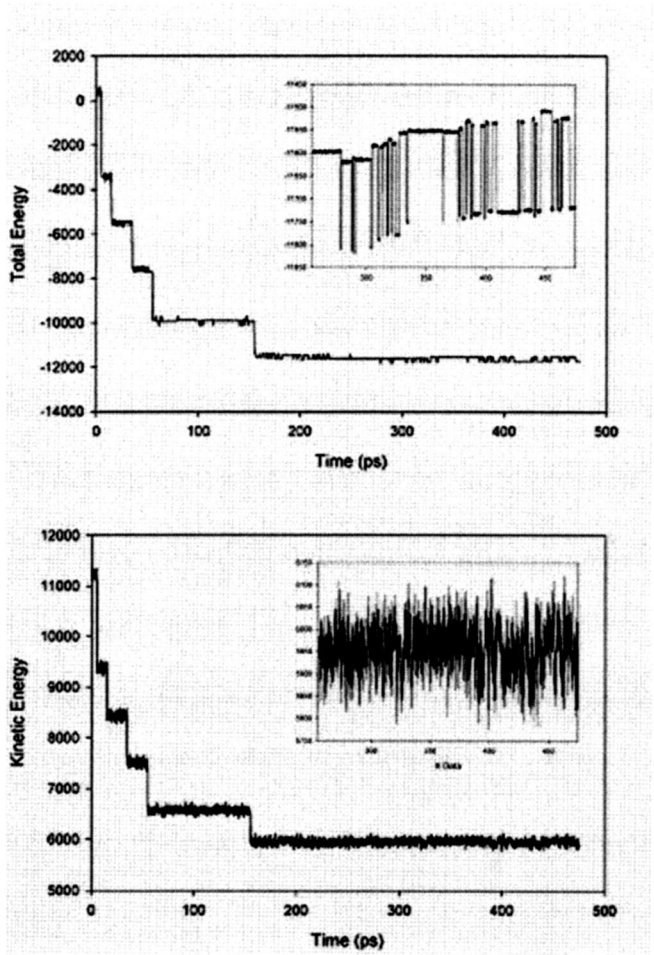

FIG. 3. Energy values are given in kcal/mol. Initial temperature is 600 K. Final temperature is 317 K.

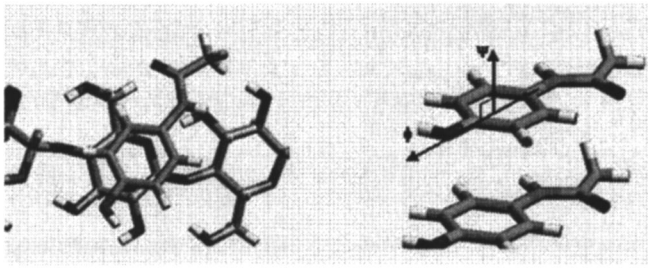

FIG. 4. The initial $(\phi=0,\psi=0)$ positions of paracetamol molecules in (left) the presence of glycogen and (right) presence of another paracetamol molecule.

$(v_{new}/v_{old})=\sqrt{(T_{target}/T_{system})}$. Velocity is updated every 100 time steps. The deviation from the canonical ensemble is small in this case and simulations carried out using other temperature control schemes produced the same results essentially. Direct velocity scaling is thus chosen because of its simplicity. Pressure and cell volume were kept constant as well. Molecular dynamics simulation was performed for 465 ps. The first 255 ps were considered as equilibration and not used to calculate any quantities. This amount of time is sufficient for the convergence of the quantities that we are interested in, such as energy (Fig. 3). Coordinates were stored to disk every 100 fs. Only data from the final 210 ps were used for analysis. A separate simulation of the smaller system comprising of only paracetamol and water molecules was carried out using the same procedures.

All simulations were performed with the Discover module in InsightII on a SGI Origin 2000 supercomputer. Visualization was carried on a SGI Octane. The jobs were run at the Supercomputing and Visualization Unit, NUS, Singapore. Each integration step takes 3.398 s. Analysis programs are written in FORTRAN.

D. Conformational mapping

Conformational mapping is a simple yet powerful method that is used to study alternative minima and conformations [5]. As it consumes less computational time than molecular dynamics, it is also a suitable method for elucidating the ordering mechanism. Unlike most conformational mappings, the energies mapped out in this case are nonbonded rather than the bonded ones such as torsional energies. This favors the use of rigid rotation which does not involve subjecting the molecules to certain constraints and reminimizing the energy.

Given the numerous degrees of freedom possessed by the paracetamol molecule, it is impossible to map out and visualize the entire conformation space. Nonetheless, it is well known that the rotation about the principal axis which give the largest or the smallest moment of inertia is stable [6]. This allows us to identify the orientational variables that play a significant role in the ordering process. These rotation axes (Fig. 4) are defined to be $\boldsymbol{\phi}=\mathbf{R}_{C3}-\mathbf{R}_{C6}$ and $\boldsymbol{\psi}=(\mathbf{R}_{C1}-\mathbf{R}_{C6})\times(\mathbf{R}_{C5}-\mathbf{R}_{C6})$ with rotation center $(\mathbf{R}_{C3}+\mathbf{R}_{C6})/2$. $\mathbf{R}_x$ in this case denotes coordinates of atom x. Computations of energy were carried out with each increment of (ϕ,ψ) of a paracetamol molecule in the presence of (a) glycogen and (b) another paracetamol molecule. The energy evaluated in the conformation maps is the nonbonding potential comprising of the van der Waals interaction and the electrostatic interaction defined by CVFF (950) [7–14].

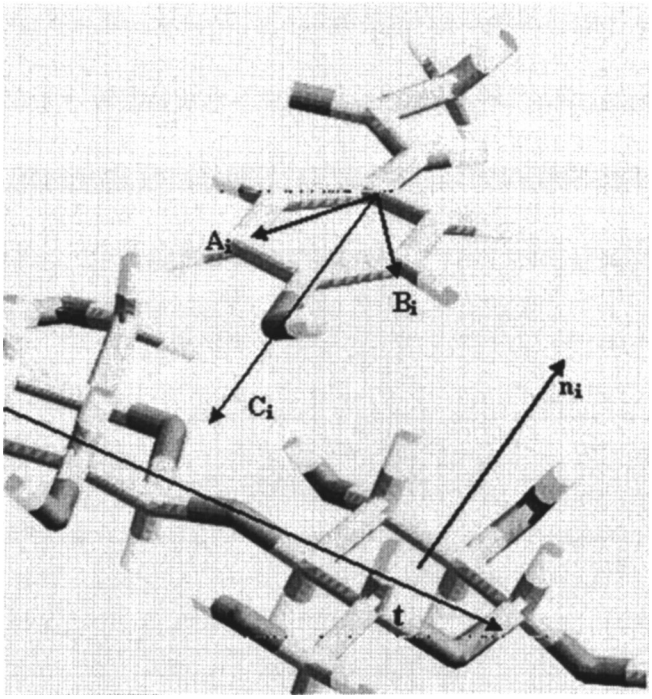

FIG. 5. Variables involved in the computation of the various order parameters. Three order parameters are required to fully characterize the orientation of the molecule. $\mathbf{n}_i$ is the normal to the plane is defined by $C1$, $C3$, and $C4$ atoms of the glycogen ring.

III. RESULTS AND DISCUSSIONS

A. Order parameter

The ordering of paracetamol molecules can be characterized by an order parameter of type [15–17]:

$$s=\tfrac{1}{2}(3\langle\cos^2\theta\rangle-1). \tag{1}$$

θ is the angle between predefined molecular axes of the glycogen chain and paracetamol molecule. $\langle\,\rangle$ denotes an ensemble average which involves averaging over all paracetamol molecules and over a time interval of 210 ps (42 consecutive data points, 5 ps apart). Time averaging helps to suppress fast noise [18]. Equation (1) is a natural extension of the order parameter defined in the original Maier-Saupe molecular model [19] of the nematic phase. In this model, the dispersion force between anisotropic molecules is proportional to $-(\frac{3}{2}\cos^2\theta_{12}-\frac{1}{2})$ where θ_{12} is the angle between the directions of the long axes of the two molecules. Using the mean field approximation, one can define the order parameter to be $s=\langle\frac{3}{2}\cos^2\theta_1-\frac{1}{2}\rangle$ where θ_1 is now the angle between the long axis of one molecule and a preferred axis in space. With this approximation, the average potential each molecule feels becomes proportional to $-(\frac{3}{2}\cos^2\theta_1-\frac{1}{2})s$. In

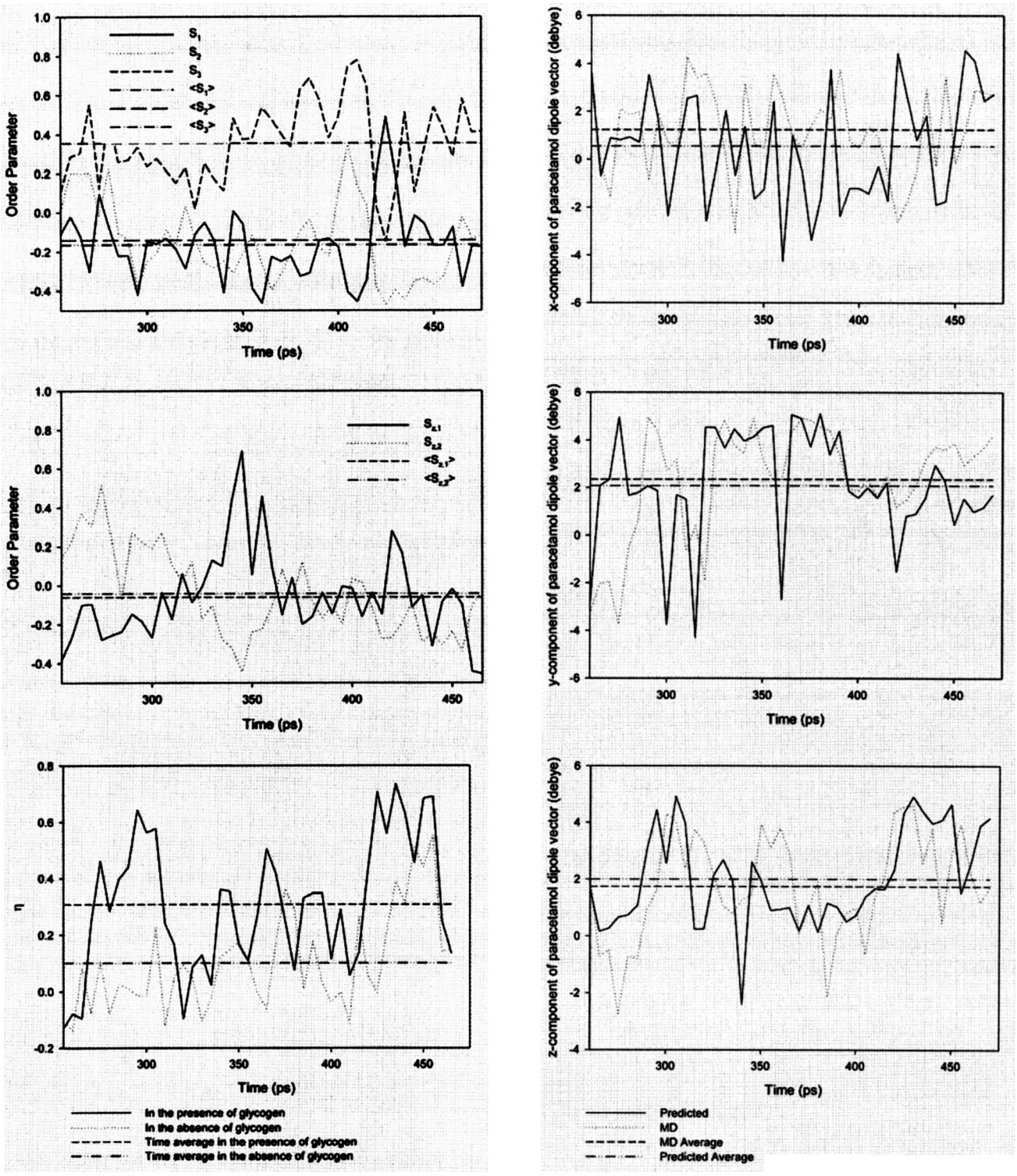

FIG. 6. Time series of order parameters and η. The definitions of the order parameters stated here are given in Eqs. (2)–(6). For perfect parallel or perpendicular alignment, $s=1$ or -0.5, respectively. For random orientation, $s=0$.

the presence of glycogen, the preferred axis is thus defined with respect to the molecular axes of the glycogen chain. We also distinguish between instantaneous order parameter and the time averaged order parameter; the instantaneous order parameter involves only the averaging of all paracetamol molecules without time averaging. It gives the order of a system of paracetamol molecules at a particular instant in time. For perfect parallel or perpendicular alignment, $s=1$ or -0.5, respectively. For random orientation, $s=0$.

Three order parameters based on different molecular axes have been selected to fully characterize the ordering of paracetamol since each parameter represents ordering in a certain direction. Alternative choices of molecular axes may be chosen but they do not alter the overall picture of the

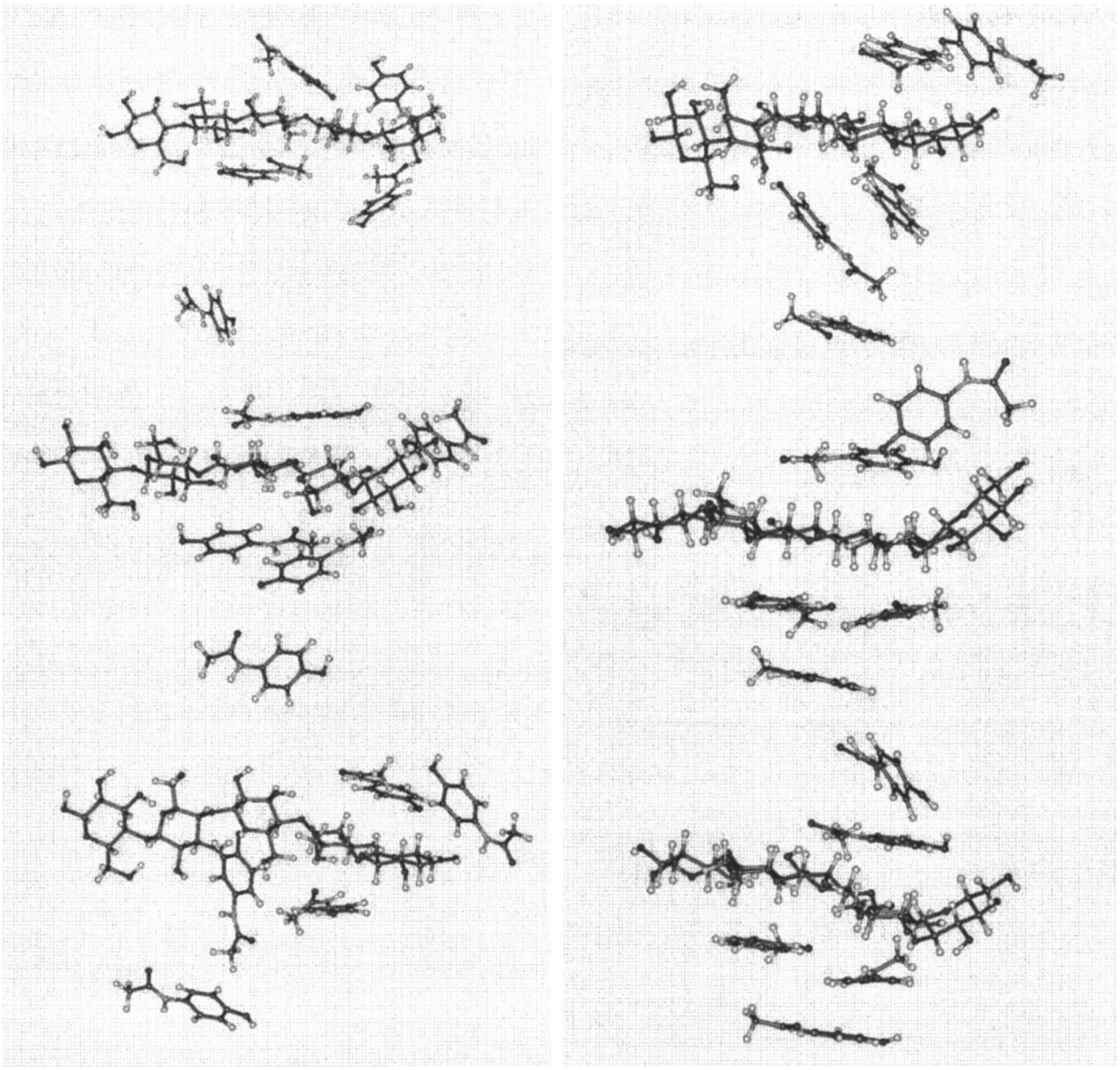

FIG. 7. Snapshots of MD simulation (from top to bottom: 255, 280, 320, 345, 380, 410 ps). Water molecules are not shown in these shots. The coordinate axes are reorientated in each snapshot to give a better view of the ordering process.

ordering process. The order parameters to be computed for a system comprising of N paracetamol molecules are as follows:

$$s_1 = \frac{3}{2}\left\{\left[\frac{1}{N}\sum_{i=1}^{N}\left[\frac{\mathbf{t}\cdot(\mathbf{A}_i\times\mathbf{B}_i)}{|\mathbf{t}||\mathbf{A}_i\times\mathbf{B}_i|}\right]^2\right]-1\right\}, \tag{2}$$

$$s_2 = \frac{3}{2}\left\{\left(\frac{1}{N}\sum_{i=1}^{N}[\hat{\mathbf{t}}\cdot\hat{\mathbf{C}}_i]^2\right)-1\right\}, \tag{3}$$

$$s_3 = \frac{3}{2}\left(\left\{\frac{1}{N}\sum_{i=1}^{N}\left[\frac{\mathbf{n}\cdot(\mathbf{A}_i\times\mathbf{B}_i)}{|\mathbf{n}||\mathbf{A}_i\times\mathbf{B}_i|}\right]^2\right\}-1\right), \tag{4}$$

where $\mathbf{n}/|\mathbf{n}|=(1/K)\Sigma_{k=1}^{K}(\mathbf{n}_i/|\mathbf{n}_i|)$. $\mathbf{n}_i$ is the normal of the plane defined by a sugar ring in the polysaccharide. As before, $\mathbf{A}_i=\mathbf{R}_{C2}-\mathbf{R}_{C6}$, $\mathbf{B}_i=\mathbf{R}_{C4}-\mathbf{R}_{C6}$ and $\mathbf{C}_i=\mathbf{R}_{C3}-\mathbf{R}_{C6}$. $\mathbf{t}$ is defined to be the vector pointing from $C4$ atom of the glycogen monomer at one end to the $C1$ atom of the glycogen monomer at the other end. Figure 5 provides a visual representation of these vectors.

In the absence of glycogen, the z axis is taken to be the axis of preferred orientation $\hat{\mathbf{m}}$:

$$s_{1,z} = \frac{3}{2}\left\{\left[\frac{1}{N}\sum_{i=1}^{N}\left[\frac{\hat{\mathbf{m}}\cdot(\mathbf{A}_i\times\mathbf{B}_i)}{|\mathbf{A}_i\times\mathbf{B}_i|}\right]^2\right]-1\right\}, \quad (5)$$

$$s_{2,z} = \frac{3}{2}\left\{\left[\frac{1}{N}\sum_{i=1}^{N}(\hat{\mathbf{m}}\cdot\hat{\mathbf{C}}_i)^2\right]-1\right\}. \quad (6)$$

In Fig. 6, we observe that the instantaneous order parameters fluctuate rapidly with time. The time averaged order parameters for the paracetamol-glycogen system are as follows: $s_1=-0.165\pm0.183$, $s_2=-0.141\pm0.196$, $s_3=0.361\pm0.194$. On the other hand, the time averaged values for the paracetamol system is $s_{1,z}=-0.061\pm0.227$ and $s_{2,z}=-0.042\pm0.223$. The error indicated here is the standard deviation. We note that the absolute values of $s_{1,z}$ and $s_{2,z}$ are one order of magnitude smaller than their respective standard deviations. This implies that at 317 K, the paracetamol molecules gain sufficient energy to assume all possible orientations, especially at low density, and the fluid becomes isotropic [20]. On the other hand, the finite but significant s_1, s_2, and s_3 implies that the paracetamol fluid undergoes a transition to a more ordered phase in the presence of glycogen at the same temperature of 317 K. This is especially interesting since we are dealing with a single polymeric strand of glycogen which provides only a small surface for any interfacial effect.

Since the intermolecular potential is proportional to $-(\frac{3}{2}\cos^2\theta_{12}-\frac{1}{2})$, it is of interest to observe how $\eta=-\langle\frac{3}{2}\cos^2\theta_{12}-\frac{1}{2}\rangle$ varies in the absence/presence of glycogen. The results are also presented in Fig. 6. The time averaged η increases by more than three times in the presence of the glycogen substrate. In other words, the tendency for paracetamol molecules to have parallel orientation of their long axes $\mathbf{C}_i$ increases with the introduction of the polysaccharide substrate. There is competition between minimization of the anisotropic intermolecular interaction (by having parallel orientation of the paracetamol molecules' long axes) and randomness at high temperatures. The introduction of a polysaccharide substrate minimizes the anisotropic interaction without altering the temperature of the system.

Figure 7 gives a visual account of the ordering process. Some observations may be made at this point. There is a tendency for the phenyl rings of paracetamol molecules to align themselves with the sugar rings of the glycogen strand while the chain tails point away from the polysaccharide strand. The snapshots also show that the paracetamol molecules do not steer away from the glycogen strand. This implies that the presence of glycogen induces an attractive potential well which traps the paracetamol molecules in it. This is an important step in the ordering process especially at higher temperatures. One reason why ordering is not observed in the control paracetamol system is the absence of such an attractive potential. From our MD simulations, we note that the mutual attraction between the paracetamol molecules is not able to bind them close to each other. At high temperatures and low density, the molecules are able to acquire enough kinetic energy to drift about with much freedom, thus allowing them to adopt nearly all possible orientations.

B. Conformational analysis

Conformation mapping results are shown in Figs. 8(a)–8(c). The contour maps in Figs. 8(a) and 8(b) share certain similarity: both show sterically repulsive barriers in the regions $100°\geqslant\phi\geqslant50°$ and $250°\geqslant\phi\geqslant300°$. There are essentially four regions in the conformation space that are accessible to the paracetamol molecule at $T=300$ K based on its average kinetic energy of 30 kT or 17.87 kcal/mol. These regions lie within the contour lines marked by 1.8, or 63.09 kcal/mol. As expected, the (ϕ,ψ) conformation space accessible to the paracetamol molecule in the presence of glycogen is more restricted. Such restricted accessibility results in a nonrandom distribution of the orientation of the paracetamol molecule, which contributes to the observed values in the order parameter. On the other hand, there exists, for instance, no restriction in the value of ψ that the paracetamol molecule can sample in the presence of another paracetamol molecule at 317 K. This results in a random distribution of C_i's that gives rise to $\langle s_2\rangle=0$ for the control model.

The contour maps shown in Figs. 8(a)–8(c) are not sufficient. The restriction in ϕ for the paracetamol-paracetamol system may seemingly imply a finite order parameter. However, as mentioned previously, the mutual attraction between paracetamol molecules are much weaker and this implies that the repulsion experienced can be reduced significantly when the paracetamol molecules are spaced further apart as a result of thermal excitation. Therefore, conclusions can only be made after extensive conformation mappings and, in certain occasions, comparisons with MD results. A series of such conformation maps (not published here) have been done and the observations from all the conformation maps [including Figs. 8(a)–8(c)] can be summarized as follows:

(1) The paracetamol molecule prefers to lie above and below the sugar rings of the glycogen strand instead of the sides.

(2) The flat aromatic ring of the paracetamol molecule prefers to stack parallel to the sugar ring.

(3) The phenylene rings are attractive while the flexible chain tails of the paracetamol molecules are repulsive. The repulsion between the chain tails of two paracetamol molecules is weak and insignificant at high temperatures.

The strong attraction between the phenylene and sugar rings therefore plays an important role in the ordering mechanism. Here, we draw parallels from the studies made on highly ordered columnar phases. The columns are formed due to an attraction between the flat aromatic cores of the disklike molecules while the fluidity of the phase is determined by the long flexible chains attached to the core [21].

The fluctuations of the instantaneous order parameters in Fig. 6 can also be related to the energy fluctuation which is proportional to $\sqrt{(2kT^2C_v)}$ where C_v can be expressed as $fk/2$ with f being the number of degrees of freedom. This follows from the fact that the distribution in energy is a Gaussian distribution centered about $\langle E(\phi,\psi)\rangle$ with a width equal to $\sqrt{(2kT^2C_v)}$ (see Ref. [22]). Consequently, if the number of molecules N is increased, the ratio $\langle E(\phi,\psi)\rangle/\sqrt{(2kT^2C_v)}\propto1/\sqrt{N}$ will decrease and the observed fluctuation should decrease correspondingly.

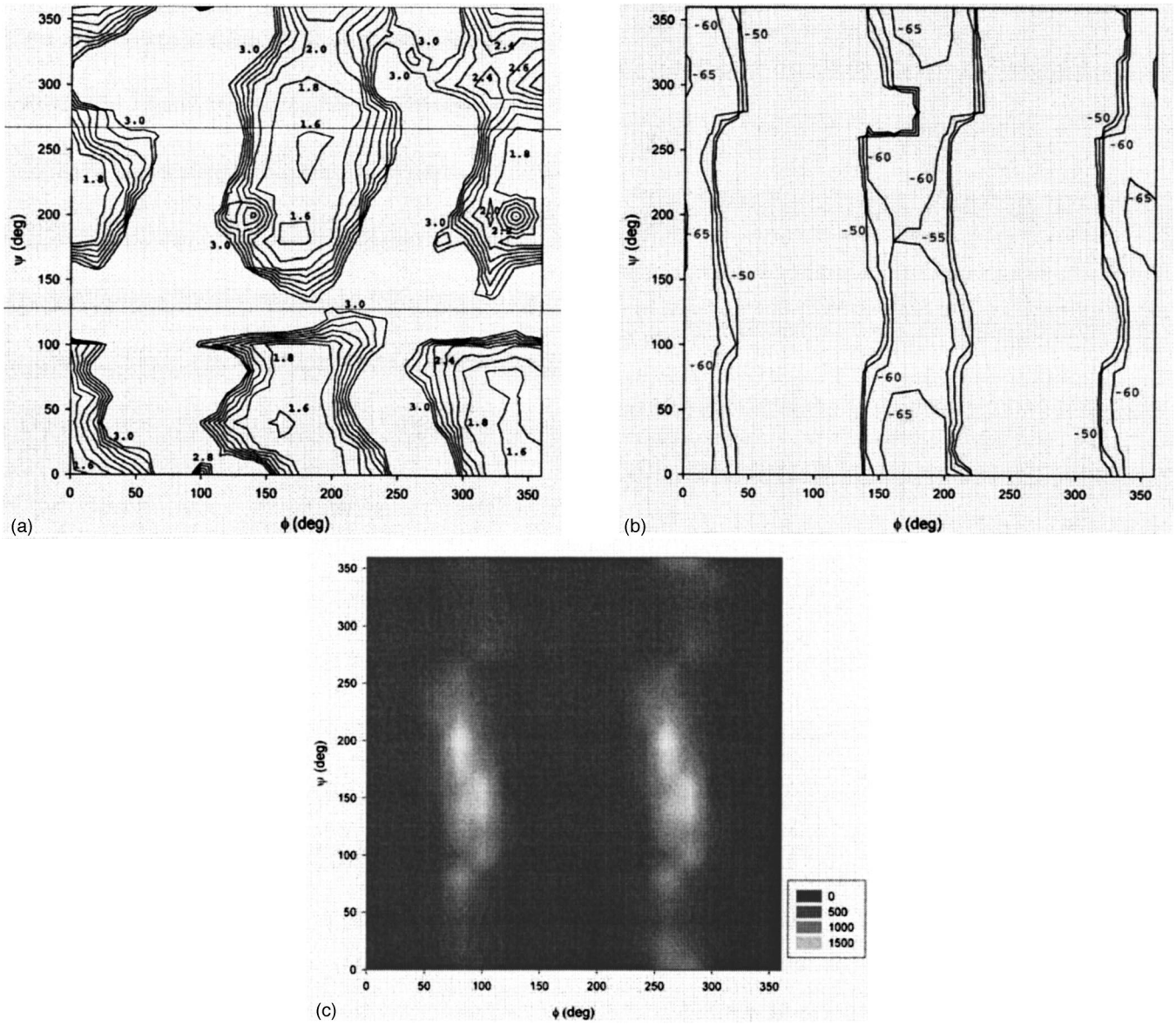

FIG. 8. (a) Conformation map for the glycogen-paracetamol system (see Fig. 3) Energy values (in kcal/mol) are represented by a logarithmic scale which is truncated at 3.0. Contour lines shown here are in increments of 0.2. (b) Conformation map for the paracetamol-paracetamol system (see Fig. 3) Energy values (in kcal/mol) are shown on a linear scale [as compared to Fig. 7(b)] which is truncated at −50 kcal/mol. Contour lines shown here are in increments of 5 kcal/mol. (c) a different range of energies. Higher energies (kcal/mol) are represented by lighter colors.

C. Dipole-induced orientational ordering

Paracetamol molecules, like any anesthetic molecules, possess a permanent electric dipole [23]. The geometric arrangement and forcefields of the polysaccharide substrate cause a certain degree of ordering of the paracetamol molecules. Moreover, the contour map in Fig. 8(a) reveals a certain degree of periodicity in energy with regard to the variables chosen. This leads us to postulate that dipole-dipole interactions play a dominant role in the ordering process. In other words, we assume that dipole interaction is the dominant term in the multipole expansion that takes into account the geometric arrangement of the polymeric substrate as well as the periodicity in potential energy. This is in contrast to the understanding that orientational ordering of molecules within liquid-crystal phases mainly arises from size and shape dependent anisotropic short-range interactions [24–26] and to a lesser extent from anisotropic long-range interactions that involve molecular dipoles, quadrupoles, and polarizabilities [27,28]. The idea of using dipole-dipole interaction has often been used in theoretical treatment of spontaneous long-range orientational order of the nematic phase in the form of a molecular field method. Born proposed a molecular field theory of the nematic state by treating the medium as an assembly of permanent electric dipoles. As in the Maier-Saupe theory, each molecule is assumed to be in an averaging orienting field due to its environment [29], in this case, the dipole field created by the polysaccharide substrate. The dipole fields due to the other

paracetamol molecules can be neglected when the density of paracetamol molecules is very low.

The dipole orientational energy between a glycogen strand and paracetamol molecule can be written as

$$U = -\boldsymbol{\mu} \cdot \left\{ \frac{1}{4\pi\varepsilon_0 r^3} [3(\mathbf{p} \cdot \hat{\mathbf{r}})\hat{\mathbf{r}} - \mathbf{p}] \right\}, \tag{7}$$

where $\boldsymbol{\mu} = (\mu \sin\theta \cos\phi, \mu \sin\theta \sin\phi, \mu \cos\theta)$ is the dipole vector of a paracetamol molecule and $\mathbf{p} = (p_x, p_y, p_z)$ is the dipole vector of glycogen.

We ignore any thermal effects in the following calculations. This is justified by the fact that thermal fluctuation can be neglected when averaged over an extended period of time. Furthermore, we are interested primarily in the short-range orientational behavior of paracetamol. Within this range, thermal effects can be neglected to a good approximation since $|U| > kT$. We also choose to neglect the dipole interactions between neighboring paracetamol molecules.

Based on these assumptions, we may calculate the direction of the dipole vector of the paracetamol molecule and compare it with simulation results. The derived dipole vector will also indicate the orientation of paracetamol. By setting $\partial U/\partial\theta$ and $\partial U/\partial\phi$ to be zero, we have

$$\tan\phi = \frac{D_y}{D_x},$$

$$\tan\theta = \frac{D_x \cos\phi + D_y \sin\phi}{D_z} \tag{8}$$

where $D_i = p_i - 3(\mathbf{p} \cdot \hat{\mathbf{r}})\hat{\mathbf{r}}_i$, $i = x, y, z$.

From the saved MD trajectory files, we compute the dipole vectors of a single paracetamol molecule (labeled 6 in Fig. 2) and the glycogen strand every 5 ps, starting from 255 up to 465 ps. The computation is carried out using the formula

$$d_a = 4.802 Q_{min}(Q^+_{COC} - Q^-_{COC}), \tag{9}$$

where 4.802 is the factor necessary to convert the value to debyes, $Q_{\min}$ is the smaller absolute value of the total positive charge and the total negative charge and d_a can refer to either p_a or $\mu_a \cdot a = x, y$ or z. The center of positive/negative charge is defined as

$$Q^{\pm}_{COC} = \sum_{j=1}^{N} (q_j r_{ja}) / \sum_{j=1}^{N} q_j. \tag{10}$$

The summations in Eq. (10) run over all positive (+) or negative (−) charges as appropriate, j is used to denote atom j and r_{ja} refers to either the x, y, or z component of the coordinates of charge j.

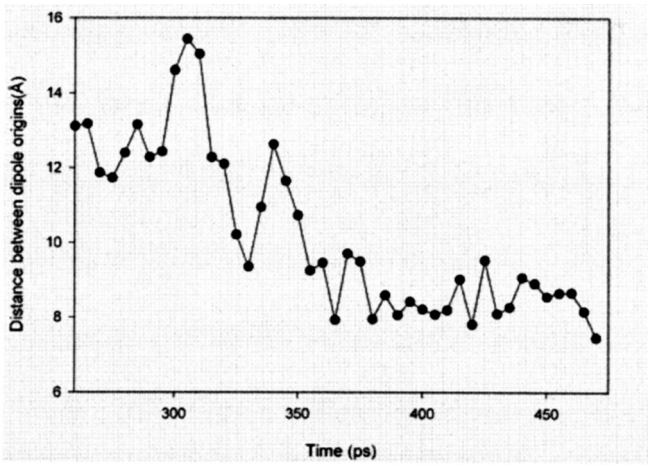

FIG. 9. Time series of dipole vector components. The black bold lines denote the dipole components calculated using Eq. (8) whereas the dashed lines refer to the dipole components calculated from the MD simulations based on Eq. (9).

Figure 9 shows the comparison between the dipole vectors calculated using Eq. (8) and the dipole vectors obtained from the MD simulation. The agreement between the predicted components and the MD results are slightly better when the distance between the dipole origins is smaller. This is to be expected based on our previous assumptions. At shorter distances, we can neglect thermal fluctuations to a good approximation.

The effect of thermal fluctuation can be reduced by taking their time averaged values. This is shown in Table II. The calculated vector components are within one standard deviation of the MD values. The calculated y and z components

TABLE II. Comparison between theory and simulation.

		Average value based on MD simulation	Average value based on Eq. (8)	Standard deviation of component as given by MD simulation
x component of	$N=21$	1.31	0.22	1.69
paracetamol	$N=43$	1.25	0.55	1.78
Dipole vector (D)				
y component	$N=21$	2.53	2.69	2.21
(D)	$N=43$	2.35	2.08	2.30
z component	$N=21$	1.39	1.81	2.02
(D)	$N=43$	1.74	2.00	1.83

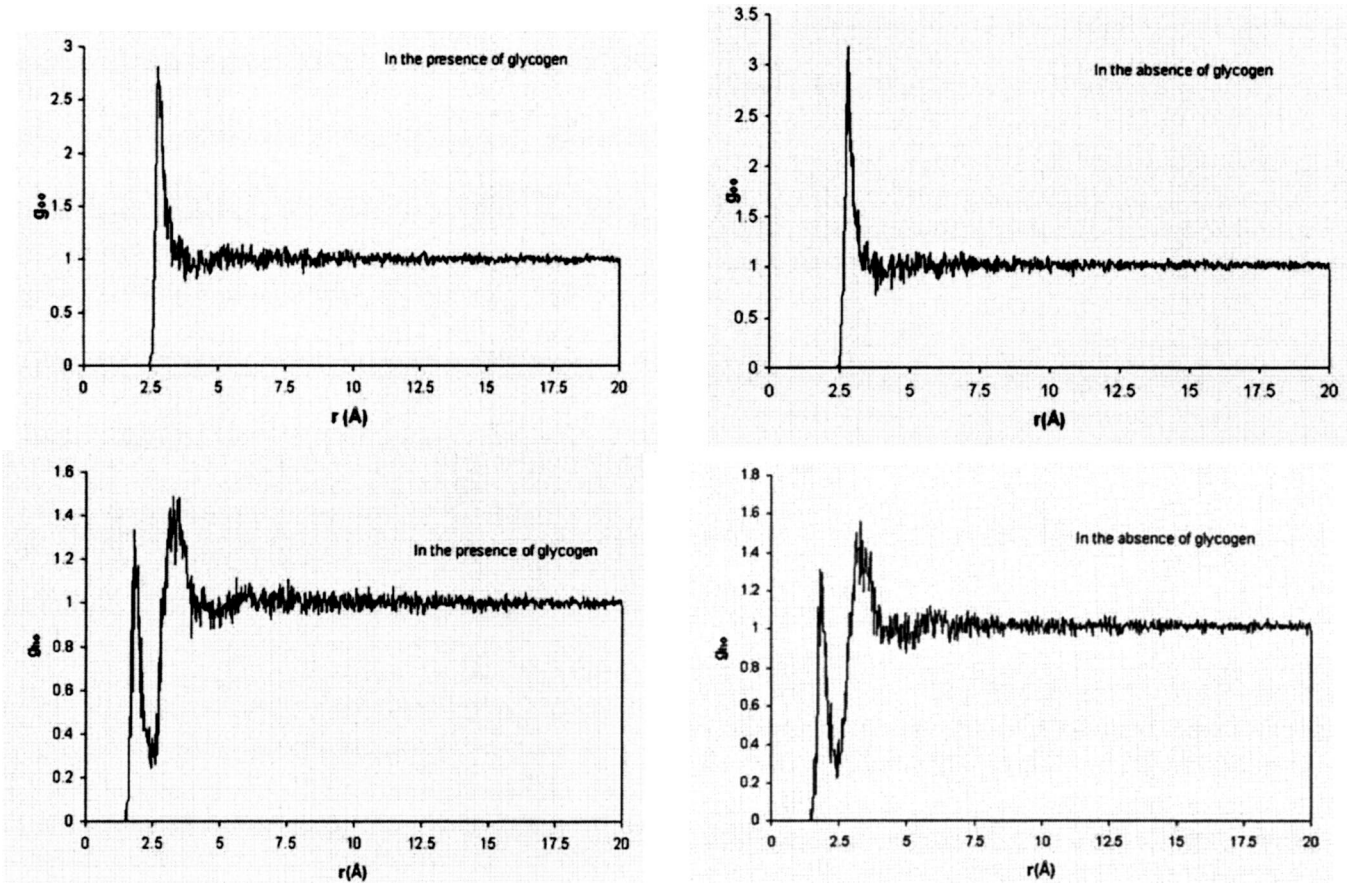

FIG. 10. Radial distribution functions g_{OO} and g_{HO} of water in the presence/absence of the glycogen substrate at 317 K.

agree well with their respective MD values. Nevertheless, the x component deviates from the MD value significantly. Increasing the number of sample points N will reduce the effects of fluctuation and give a better time averaged estimate with a smaller standard error. This is also shown in Table II where the predicted x component agrees better with the corresponding MD value when N is increased to 43 (readings are taken every 5 ps) from 21 (readings are taken every 10 ps). However, the percentage difference between the predicted x-component value and the corresponding MD result remains significant (56.0%). The percentage difference of the predicted y and z-component values and the MD results lies in the range of 10%–15%. To account for this discrepancy, one should take a further look at the assumptions stated at the beginning. First of all, while it is true that the overall density of paracetamol molecules is low, the local density is high. As a result, one has to take into account the interaction of neighboring paracetamol molecules using molecular field approximation. Second, the dipole vector of a paracetamol molecule is sensitive to relative positions of certain groups of atoms such as the hydroxyl, carbonyl, and the terminal methyl groups. Large and rapid motions of these groups at room temperature will alter the direction of the vector even though the entire molecule may not be moving much. To remove this source of discrepancy, one can repeat the simulation by applying structural constraints on the molecules. Last but not least, Eq. (8) represents mechanical equilibrium whereas the average we are considering is thermal equilibrium. The discrepancy due to this is small compared to the above-mentioned factors.

As a side note, the thermal contributions to the paracetamol dipole orientation can be included by evaluating the following integrals:

$$\langle \mu_x \rangle = \frac{\int_0^{2\pi}\int_0^{\pi} \mu \sin^2\theta \cos\phi \exp(-U/kT) d\theta d\phi}{\int_0^{2\pi}\int_0^{\pi} \exp(-U/kT)\sin\theta d\theta d\phi},$$

$$\langle \mu_y \rangle = \frac{\int_0^{2\pi}\int_0^{\pi} \mu \sin^2\theta \sin\phi \exp(-U/kT) d\theta d\phi}{\int_0^{2\pi}\int_0^{\pi} \exp(-U/kT)\sin\theta d\theta d\phi},$$

$$\langle \mu_z \rangle = \frac{\int_0^{2\pi}\int_0^{\pi} \mu \sin\theta \cos\theta \exp(-U/kT) d\theta d\phi}{\int_0^{2\pi}\int_0^{\pi} \exp(-U/kT)\sin\theta d\theta d\phi}, \quad (11)$$

with U given by Eq. (7). This treatment is essentially based on the canonical ensemble of N weakly interacting particles, in this case, paracetamol molecules. We have also assumed that the radial distance between the dipole vectors is constant

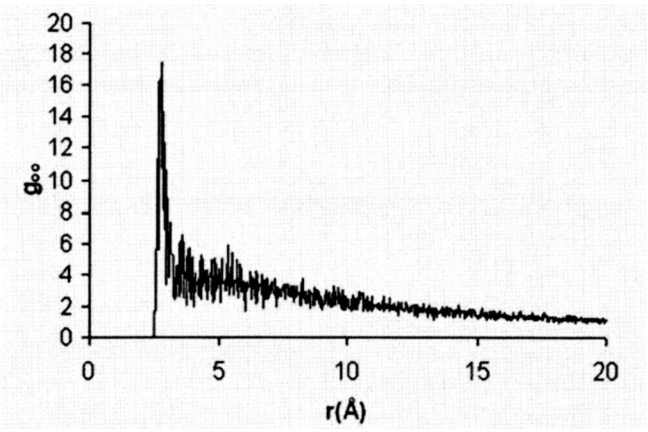

FIG. 11. Radial distribution function g_{OO} of water in the vicinity of the glycogen substrate. Only water molecules within a sphere of radius=15 Å centered at the middle of the glycogen substrate are selected to calculate the distribution function.

to simplify the integrals. Nevertheless, the analytical solutions to the integrals are extremely difficult to obtain. One can certainly seek a numerical solution to the Eq. (11), but this is beyond the scope of our present discussion.

D. Role of solvent in the preordering process

Understanding the role of water solvent in a preordering process such as this can begin with the analysis of the OO and HO radial distribution functions g_{OO} and g_{HO} in the absence/presence of the glycogen substrate are shown in Fig. 10. The calculated g_{HO} remains nearly identical when glycogen is introduced into the paracetamol-water system. On the other hand, the height of the first peak of g_{OO} decreases in the presence of glycogen, indicating weaker structure of liquid water. The solvent is also more structured in the vicinity of the glycogen substrate (Fig. 11). How this affects the ordering of paracetamol molecules is not fully understood and remains a topic of further investigation.

IV. CONCLUDING REMARKS

The investigations carried out in this paper can be generalized to a much larger class of anesthetics and polysaccharides since one can also expect a strong attraction between the aromatic cores of the anesthetic molecules and the sugar rings of the polysaccharides.

The polysaccharide used in the experiments carried out by Liu is not a single strand that we modeled here. It is a polymer matrix whose exact structure has not been fully comprehended [30,31]. We choose to work with a single strand so as to better elucidate the interactions between the polymer substrate and the paracetamol molecules. The use of a polymer matrix in the simulation will unnecessarily complicate the analysis. This is also one of the reasons why we choose to work with a small number of paracetamol molecules. However, in light of the fact that dipolar interactions play an important role in the ordering process, we can modify the model prescribed by Eq. (8) to include the effects of a polysaccharide matrix by treating it as a dipole array so that $D_i=\Sigma_{\alpha=1}^{N}p_{i,\alpha}-3\Sigma_{\alpha=1}^{N}(\mathbf{p}\cdot\hat{\mathbf{r}})_{\alpha}\hat{r}_{i,\alpha}$. N is the number of polysaccharide strands in the matrix and each strand represents one dipole. Similarly, as the number of paracetamol molecules increase, neighbor correlations become significant.

The significance of the dipole orientation effect as demonstrated in this paper dictates the type of polymeric substrate that can be used to initiate the preordering process. The dipole moments of each monomer must try to align themselves vectorially to give the maximal dipole moment possible. A large substrate dipole moment will result in a highly ordered phase. In the case of anesthetic molecules, another criterion the substrate must have is the disklike surface. The disks are natural sites for ordering of anesthetic molecules since the ordering is partly driven by the attractive aromatic cores. Polysaccharides fit the above-mentioned criteria. Nonetheless, an important application of ordering using a substrate lies in the crystallization of complex molecules. To be incorporated into the crystal structure, fluid molecules at the kink sites of the embryos must adopt a required orientation and conformation and not just any orientation. Consequently, the direction of the dipole vector of the polymeric substrate becomes a very crucial criterion. It can either lead to an easier incorporation of growth units into the crystal structure at kink sites or increased difficulty of rearrangement to the crystalline order, thereby increasing the conformational and orientational free energy. A precursor to the selection of a suitable substrate will therefore involve accurate calculations of the dipole vector of the polymer and anesthetic molecules.

[1] X. Y. Liu, Appl. Phys. Lett. **79**, 39 (2001).
[2] X. Y. Liu, J. Phys. Chem. B **105**, 11550 (2001).
[3] CVFF is provided with Discover in InsightII, Release 2000.
[4] Ivan G. Binev, Pavlina Vassileva-Boyadjieva, and Yuri I. Binev, J. Mol. Struct. **447**, 235 (1998).
[5] Bruce R. Gelin, *Molecular Modeling of Polymer Structures and Properties* (Hanser/Gardner, New York, 1994), p. 48.
[6] T. W. B. Kibble and F. H. Berkshire, *Classical Mechanics* (Addison Wesley Longman, London, 1985), p. 177.
[7] A. T. Hagler, E. Huler, and S. Lifson, J. Am. Chem. Soc. **96**, 5319 (1974).
[8] A. T. Hagler and S. Lifson, J. Am. Chem. Soc. **96**, 5327 (1974).
[9] S. Lifson, A. T. Hagler, and P. Dauber, J. Am. Chem. Soc. **101**, 5111 (1979).
[10] A. T. Hagler, S. Lifson, and P. Dauber, J. Am. Chem. Soc. **101**, 5122 (1979).
[11] A. T. Hagler, P. Dauber, and S. Lifson, J. Am. Chem. Soc. **101**, 5131 (1979).
[12] D. H. Kitson and A. T. Hagler, Biochemistry **27**, 7176 (1988).

[13] D. H. Kitson and A. T. Hagler, Biochemistry **27**, 7176 (1988).
[14] P. Dauber, V. A. Roberts, D. J. Osguthorpe, J. Wolff, M. Genest, and A. T. Hagler, Proteins: Struct., Funct., Genet. **4**, 31 (1988).
[15] Xiang-Yang Liu and P. Bennema, Phys. Rev. E **48**, 2006 (1993).
[16] M. A. R. B. Castanho, S. Lopes, and M. Fernandes, Spectroscopy (Amsterdam) **17**, 377 (2003).
[17] S. Chandrasekhar, *Liquid Crystals*, 2nd ed. (Cambridge University Press, Cambridge, 1992), Chap. 2, p. 38.
[18] Yuji Takaoka, Marta Pasenkiewicz-Gierula, Hiroh Miyagawa, Kunihiro Kitamura, Yoshiyasu Tamura, and Akihiro Kusumi, Biophys. J. **79**, 3118 (2000).
[19] W. L. McMillan, Phys. Rev. A **4**, 1238 (1971).
[20] S. Chandrasekhar, *Liquid Crystals*, 2nd ed. (Cambridge University Press, Cambridge, 1992), Chap. 2, p. 31.
[21] Mikhail A. Osipov and Joachim Stelzer, Phys. Rev. E **67**, 061707-1 (2003).
[22] Kerson Huang, *Statistical Mechanics*, 2nd ed. (Wiley, New York, 1987), p. 147.
[23] G. A. Isaeva, A. V. Dmitriev, and P. P. Isaev, Biophysics (Engl. Transl.) **45**, 1034 (2000).
[24] W. Gelbart, J. Phys. Chem. **86**, 4289 (1982).
[25] D. Frenkel, Liq. Cryst. **5**, 929 (1989).
[26] A. Terzis, C. Poon, E. Samulski, Z. Luz, R. Poupko, H. Zimmermann, K. Müller, H. Toriumi, and D. Photinos, J. Am. Chem. Soc. **118**, 2226 (1996).
[27] D. Photinos, E. Samulski, and H. Toriumi, J. Phys. Chem. **94**, 4694 (1990).
[28] D. Photinos, C. Poon, E. Samulski, and H. Toriumi, J. Phys. Chem. **96**, 8176 (1992).
[29] P. G. De Gennes and J. Prost, *The Physics of Liquid Crystals* (Clarendon Press, Oxford, 1993), p. 66.
[30] P. G. Righetti, Marcella Chiari, Elena Casale, Claudia Chiesa, Tikam Jain, and Robert Shorr, J. Biochem. Biophys. Methods **19**, 37 (1989).
[31] P. G. Righetti, J. Biochem. Biophys. Methods **19**, 1 (1989).